Modeling and Set Point Control of Closed-Chain Mechanisms: Theory and Experiment

Fathi H. Ghorbel, *Senior Member, IEEE*, Olivier Chételat, Ruvinda Gunawardana, and Roland Longchamp, *Member, IEEE*

***Abstract*—In this paper we derive a reduced model, that is, a model in terms of independent generalized coordinates, for the equations of motion of closed-chain mechanisms. We highlight the fact that the model has two special characteristics which make it different from models of open-chain mechanisms. First, it is defined locally in the generalized coordinates. We therefore characterize the domain of validity of the model in which the mechanism satisfies the constraints and is not in a singular configuration. Second, it is an implicit model, that is, parts of the equations of motion are not expressed explicitly. Despite the implicit nature of the equations of motion, we show that closed-chain mechanisms still satisfy a skew symmetry property, and that proportional derivative (PD)-based control with so-called simple gravity compensation guarantees (local) asymptotic stability. We discuss the computational issues involved in the implementation of the proposed controller. The proposed modeling and PD control approach is illustrated experimentally using the Rice planar delta robot which was built to experiment with closed-chain mechanisms.**

***Index Terms*—Closed kinematic chains, experimental validation, parallel robots, PD control, reduced model, simple gravity compensation.**

I. Introduction

MANY of the kinematic chains that are popular today have the links connected sequentially starting from a fixed base. The last link in the chain is connected from one end to a previous link but is free from the other end resulting in an open link chain or "open kinematic chain." Typically, each link is connected to the previous link in the link chain by a joint (revolute, prismatic, or spherical) and all of the joints are actuated. In the robotics literature, we usually refer to open kinematic chains as "serial robots." Some kinematic chains differ from this structure in which the links are connected in series as well as in parallel combinations forming one or more closed-link loops. We will refer to these mechanisms as "closed kinematic chains" or "closed-chain mechanisms." Typically, not all joints of closed-chain mechanisms are actuated. In the robotics literature, we refer to these mechanisms as "parallel robots." The simplest characterization of this class is that of the so-called fully parallel robots [44] which consist of a set of serial links each connected to a fixed base from one end, and connected to a common moving platform on the other end resulting in a closed-chain mechanism. Fig. 1 shows planar examples of an open kinematic chain (serial robot) and a closed kinematic chain (parallel robot). For closed-chain mechanisms, the actuators are typically placed lower (closer to the base or on the base itself) in the link chain. This makes the moving parts lighter which can lead to greater efficiency and faster acceleration at the end-effector. Closed-chain mechanisms offer also greater rigidity to weight ratio. Therefore, they are more suitable for fast assembly lines. Many mechanical systems, such as slider-cranks, are inherently closed-chain mechanisms. On the other hand, many other designs are intentionally built with closed-chains because of the favorable mechanical properties they offer over systems with open-chain structure. Among the early closed-chains, the Stewart platform [56] is the most popular one. It has been used as a basis for designing many robotic applications including flight simulators and some robotic machining applications. Other popular closed-chain mechanisms include the Swiss 3-degree of freedom (dof) Delta robot [9], and its French/Japanese extension the 6-dof Hexa robot [51].

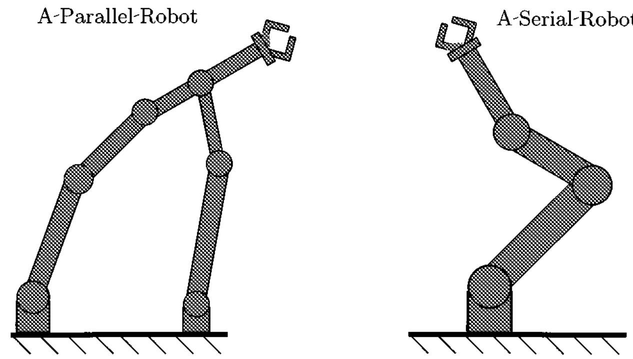

Fig. 1. Planar parallel robot and a planar serial robot.

For open-chain mechanisms, there exists in the dynamics and robotics literature a well established formulation of the equations of motion [26], [55] and a wealth of control results have been developed during the last two decades (see [1] and [48] for recent surveys). In the absence of friction and other disturbances, the standard model for the dynamics of an open-chain mechanical system not in contact with the external environment, can be obtained using for example Lagrangian dynamics [26] and is given by the following set of ordinary differential equations [55]:

$$D(\boldsymbol{q})\ddot{\boldsymbol{q}} + C(q, \dot{\boldsymbol{q}})\dot{\boldsymbol{q}} + \boldsymbol{g}(\boldsymbol{q}) = \boldsymbol{u} \tag{1}$$

Manuscript received January 16, 1998. This work was supported in part by the National Science Foundation under Grant CMS-9900194. Recommended by Associate Editor, D. Gruver.

F. H. Ghorbel and R. Gunawardana are with the Department of Mechanical Engineering, Rice University, Houston, TX 77005 USA (e-mail: ghorbel@rice.edu).

O. Chételat and R. Longchamp are with the Institut d'Automatique, Ecole Polytechnique Fédérale de Lausanne, CH-1015 Lausanne, Switzerland (e-mail: longchamp@ia.epfl.ch).

Publisher Item Identifier S 1063-6536(00)02963-8.

where[1]

$\boldsymbol{q} \in \Re^n$	vector of link positions;
$D(\boldsymbol{q})$	$n \times n$ inertia matrix;
$C(\boldsymbol{q}, \dot{\boldsymbol{q}})\dot{\boldsymbol{q}}$	represents the Coriolis and centrifugal terms;
$\boldsymbol{g}(\boldsymbol{q})$	represents the gravitational terms;
$\boldsymbol{u}$	input torque.

Note that the equations of motion defined in (1) above have the following properties.

1) The number of second-order differential equations in (1), namely n, corresponds to the number of dof of the open-chain system.
2) All elements of (1) are defined *explicitly*.
3) The domain of definition of the generalized coordinate $\boldsymbol{q}$ in (1) is the whole n-dimensional real space, i.e., $\boldsymbol{q} \in \Re^n$.

Along with these properties, the equations of motion above have other fundamental properties that have been fully exploited to facilitate control system design [19]. These properties consist of first the symmetry, positive definiteness and the boundedness of the inertia matrix $D(\boldsymbol{q})$ [21]–[24], and the boundedness of $D(\boldsymbol{q})^{-1}$, second the existence of an independent control input for each dof, third the linearity in parameters of (1), and fourth the skew symmetry of $\dot{D}(\boldsymbol{q}) - 2C(\boldsymbol{q}, \dot{\boldsymbol{q}})$ for a suitable choice of $C(\boldsymbol{q}, \dot{\boldsymbol{q}})$, a consequence of which is the passivity of the map $\boldsymbol{u} \rightarrow \dot{\boldsymbol{q}}$. A full spectrum of control laws have been generated during the last decade using the above model while fully exploiting the properties above. Note that most of these control laws were designed to insure *global* stability properties thanks to property G3 above.

Unlike open-chain mechanisms, the derivation of dynamic equations of motion for closed-chain mechanisms suitable for controller design is still a research topic because of the complexity of the kinematics and dynamics analyses.

The literature on the derivation of dynamic equations of motion of closed-chain mechanisms falls into three categories. In the first category, the equations of motion are derived for a particular closed-chain or a closed-chain with a specific structure [15]–[17], [25], [27], [30], [39], [40], [52]. For these special closed-chains, it is often possible to derive explicit closed-form equations of motion in terms of the actuated joint variables which are usually equal to the number of degrees of freedom. Hence, the resulting dynamic equations are similar to open-chain equations of motion, (1), with identical properties except property G3. In this case the domain of definition of the generalized coordinate $\boldsymbol{q}$ is a compact (i.e., bounded and closed) set corresponding to a subset of the workspace that is free of structural singularities. It follows that in this case, all the control laws for open-chain mechanisms are applicable to closed-chain mechanisms with the only difference that the guaranteed (Lyapunov) stability conclusions will at best be local.

In the second category, the equations of motion are derived for general closed-chain structures but they are mostly suited for simulation and computation of the dynamic terms and are not best suited for model-based control design [7], [8], [31],[33], [41], [42], [46], [54], [65]. A popular method to derive such equations of motion, which originated from the work of Wittenburg [66], is to first virtually cut open the closed-chains at joints that are not actuated and then derive the equations of motion of the resulting open-chains. If the closed-chain mechanism has n dof, then suppose the number of differential equations for the corresponding open-chains is $n' > n$. The latter (differential) equations along with the $n' - n$ (algebraic) holonomic constraints corresponding to the virtually cut joints then constitute the full equations of motion of the n dof closed-chain expressed as a set of differential algebraic equations (DAEs). After elimination of the Lagrange multipliers originating from the constraints in the full equations, a set of n' differential equations results. In this context, the difficulty of extending the existing wealth of control laws of open-chains to closed-chains lies in the fact that we end up with a number of differential equations larger than degrees of freedom, and hence the extension is not trivial.

In the third category, effort is made to generate for general n dof closed-chains exactly n second-order nonlinear differential equations similar to (1). The first attempt to propose this approach is attributed to Uicker [62] who formulated this problem for general closed chains. He first formulated the equations of motion in terms of, say n', dependent generalized coordinates and then eliminated $n' - n$ holonomic constraints to end up with n independent differential equations with n independent generalized coordinates corresponding to the number of dof of the closed-chains. He clearly noted that getting n *explicit* differential equations is impossible in general because the relationship between the dependent and independent generalized coordinates, referred to in his work as "loop equations," is not an explicit one and must be solved for by an iteration process. More recent related work includes [45]–[47] where the conclusions of Uicker [62] were reemphasized. In particular, [45] realized the possible extension of existing open-chain control strategies to closed-chains if the "loop equations" can be explicitly solved.

The literature on the control of closed-chain mechanisms includes basically two classes of results. The first class consists of nonmodel based control laws such as proportional integral derivative (PID) control [2], [34], [57], artificial intelligence-based methods [5], [6], [18], force feedback control [36], [43], [57], and teleoperator assisted hybrid control [3]. Of course, no guarantee of stability and performance can be expected from the previous approaches. The second class includes model-based control laws in which two special results are available. The first consists of control laws that are devised for special closed-chain structures for which explicit equations of motion exist; examples include optimal control [38], learning control [35], and other [60]. The second consists of controllers devised for general closed-chain mechanisms for which the "loop equation" is assumed, without justification, to be solvable explicitly. An example is the adaptive control law of [64].

In this paper, we exploit the fundamental idea of Uicker [62] to obtain a formulation of the dynamics equations of closed-chain mechanisms in terms of independent generalized coordinates, which we will refer to in this paper as "reduced

[1]In the following discussions $\Re$ denotes the set of real numbers, $\Re^n$ is the usual n-dimensional vector space over $\Re$, and $\Re^{n \times m}$ denotes the set of all $n \times m$ matrices with real elements. A neighborhood of a point $\boldsymbol{x}_0 \in \Re^n$, denoted $\mathcal{N}_{\boldsymbol{x}_0}$, is an open set in $\Re^n$ containing the point $\boldsymbol{x}_0$.

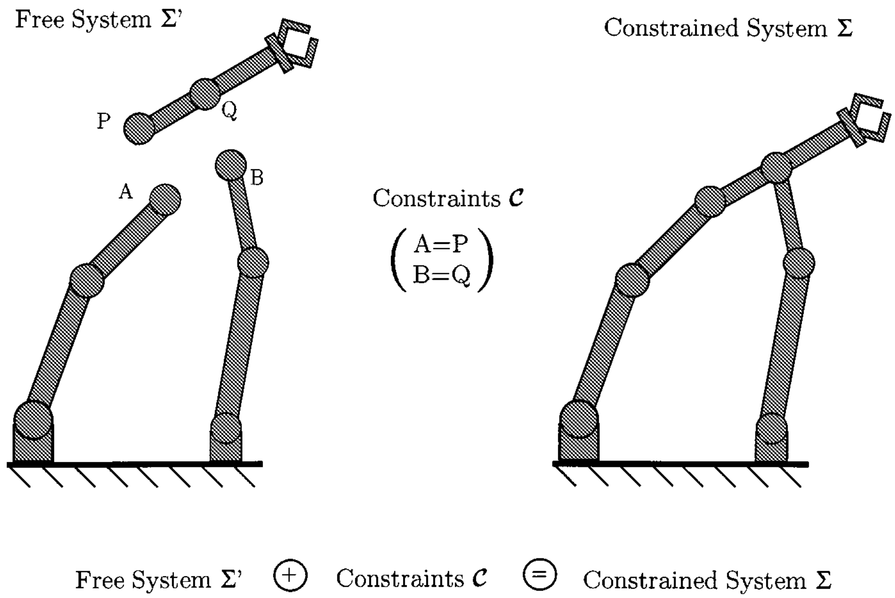

Fig. 2. Free system, constraints, and constrained system.

model." The usefulness of this formulation is in its ability to allow for the extension of model-based advanced control law designs of open-chains to closed-chains. We particularly show in this paper that the developed "reduced model" has two fundamental properties which make it different from the familiar dynamics models of open-chains [see (1)]. First, it is defined locally in the generalized coordinates $\boldsymbol{q}$ in a compact set domain with boundaries that are not easily characterizable in general. One contribution of this paper is the characterization of the boundaries of this domain using results from the Kantorovich theorem [58]. The characterization of the boundaries of the domain of definition of the equations of motion is a prerequisite to properly perform control law design and stability analysis. The second property of the equations of motion of closed-chain mechanisms is that they are implicit because of the implicit nature of the "loop equations." This gives rise to a new challenge in control law design, implementation and stability analysis as the implicit part of the dynamic model needs, for model-based controllers, to be computed on-line using numerical iterations, and furthermore the computation needs to be almost instantaneous with guaranteed convergence. Any successful control design needs to take these two special properties into consideration. We show in this paper, thanks to a skew symmetry property we prove, that PD with the so-called simple gravity compensation, evades the on-line numerical computations, and guarantees Lyapunov asymptotic stability for any general closed kinematic chain mechanism. The results of this paper are finally illustrated using an experimental closed-chain mechanism.

This paper is organized as follows. In Section II, we outline the formulation of the equations of motion of closed-chain mechanisms and highlight the special properties of the model and its fundamental differences with respect to the equations of motion of open-chain mechanisms. Furthermore we explicitly characterize the boundaries of the domain of definition of the equations of motion. In Section III, we prove a skew symmetry property and show that PD with so-called simple gravity compensation guarantees asymptotic stability for general closed-chain mechanisms. In Section IV, we illustrate the modeling and control results of the paper using the experimental Rice planar delta robot. Finally in Section V, conclusions are drawn.

II. Dynamics Model Development

A. Problem Formulation

Let an n' dof holonomic mechanical multibody system Σ' consist of a collection of rigid bodies described by the following differential equation:

$$\Sigma': \quad D'(q')\ddot{\boldsymbol{q}}' + C'(q', \dot{\boldsymbol{q}}')\dot{\boldsymbol{q}}' + \boldsymbol{g}'(\boldsymbol{q}') = 0 \tag{2}$$

where $\boldsymbol{q}' \in \boldsymbol{\Omega}' \subseteq \Re^{n'}$. $\boldsymbol{q}'$ is a vector of the generalized coordinates, $D'(\boldsymbol{q}') \in \Re^{n' \times n'}$ is the inertia matrix, $C'(\boldsymbol{q}', \dot{\boldsymbol{q}}')\dot{\boldsymbol{q}}' \in \Re^{n'}$ represent the centrifugal and Coriolis terms, and $\boldsymbol{g}'(\boldsymbol{q}') \in \Re^{n'}$ is the gravity vector. The holonomic system Σ' will be called the *free system*. It represents either a collection of several blocks of interconnected open-chain rigid-body subsystems, or a collection of free (unconstrained) rigid bodies in which case the inertia matrix D' is constant and block diagonal, and C' is the null matrix (see Fig. 2).

We now consider constraints applied at the free system and assume the following:

Assumption II.1: Assume we represent the constraints by $(n' - n)$ independent scleronomic holonomic constraints given by

$$\mathcal{C}: \quad \phi(\boldsymbol{q}') = 0 \tag{3}$$

where $\phi(\boldsymbol{q}')$ is at least twice continuously differentiable.

Note II.1: A consequence of Assumption II.1 is that $\phi_{\boldsymbol{q}'}(\boldsymbol{q}') \stackrel{\Delta}{=} (\partial\phi/\partial\boldsymbol{q}')(\boldsymbol{q}')$ is of full $(n' - n)$ rank, a property which will be exploited in the paper.

With the introduction of the constraints (3), the generalized coordinates $\boldsymbol{q}'$ are restricted to a subspace of $\boldsymbol{\Omega}'$, namely, $\boldsymbol{q}' \in \boldsymbol{U}'$ where

$$\boldsymbol{U}' \triangleq \{\boldsymbol{q}' \in \boldsymbol{\Omega}': \quad \phi(\boldsymbol{q}') = 0\} \subset \boldsymbol{\Omega}'. \tag{4}$$

It follows from standard results in analytical dynamics [26] that the free system Σ' (2), with imposed constraints $\mathcal{C}$ (3), has n-dof, and hence there exist n independent generalized coordinates $\boldsymbol{q} \in \boldsymbol{\Omega}$, where $\boldsymbol{\Omega} \subset \Re^n$, such that the system can be written in a reduced form as follows (see Fig. 2):

$$\Sigma: \quad D(\boldsymbol{q})\ddot{\boldsymbol{q}} + C(\boldsymbol{q}, \dot{\boldsymbol{q}})\dot{\boldsymbol{q}} + \boldsymbol{g}(\boldsymbol{q}) = 0 \tag{5}$$

where

$D(\boldsymbol{q}) \in \Re^{n\times n}$	inertia matrix;
$C(\boldsymbol{q}, \dot{\boldsymbol{q}})\dot{\boldsymbol{q}} \in \Re^n$	centrifugal and Coriolis vector;
$\boldsymbol{g}(\boldsymbol{q}) \in \Re^n$	gravity vector.

Remark II.1: In many situations, we may be able to choose the generalized coordinates to coincide with the variables of the actuated joints in which case the equations of motion (5) can be written as

$$D(\boldsymbol{q})\ddot{\boldsymbol{q}} + C(\boldsymbol{q}, \dot{\boldsymbol{q}})\dot{\boldsymbol{q}} + \boldsymbol{g}(\boldsymbol{q}) = \boldsymbol{u} \tag{6}$$

where $\boldsymbol{u} \in \Re^n$ is the applied generalized force vector.

The reduced model (5) or (6) of the constrained system Σ look similar to the equations of motion of standard open-chain interconnected rigid bodies, (1). For this reason, we focus in this section on ways of getting the reduced model representation (5) of the constrained system Σ using the corresponding dynamics (2) of the free system Σ' and the constraints $\mathcal{C}$ (3). Our purpose in this section is therefore to use the given information about the free system Σ' and the constraints $\mathcal{C}$ and derive the reduced model Σ and characterize its domain $\boldsymbol{\Omega}$.

B. Dependent and Independent Generalized Coordinates

The dependent generalized coordinates $\boldsymbol{q}'$ with which we initially described the free system, as given by (2), are in general readily visual. For example, they may represent the joint variables (angles and displacements) of a link, the Cartesian coordinates of its center of gravity, or its orientation. The independent generalized coordinates $\boldsymbol{q}$ with which we would like to describe the constrained system (5) can be chosen to satisfy the following twice continuously differentiable parameterization:

$$\begin{aligned} \alpha: \quad \boldsymbol{U}' &\longrightarrow \boldsymbol{U} \subset \Re^n \\ \boldsymbol{q}' &\longmapsto \boldsymbol{q} = \alpha(\boldsymbol{q}'). \end{aligned} \tag{7}$$

The parameterization (7) is usually easy to obtain explicitly. For example, and since the constrained system Σ has n-dof, we may simply pick appropriate n components of the vector $\boldsymbol{q}'$. In general, we may prefer to choose the components of $\boldsymbol{q}'$ which correspond to the variables of the actuated joints. In such cases, we can write $\boldsymbol{q} = A\boldsymbol{q}'$, where A is a constant matrix operator which "picks" the needed components of $\boldsymbol{q}'$.

Using the constraint (3) and the parameterization (7) we write

$$\begin{bmatrix} \phi(\boldsymbol{q}') \\ \alpha(\boldsymbol{q}') \end{bmatrix} = \begin{bmatrix} 0 \\ \mathrm{q} \end{bmatrix} \tag{8}$$

and define

$$\psi(\boldsymbol{q}') \triangleq \begin{bmatrix} \phi(q') \\ \alpha(\boldsymbol{q}') \end{bmatrix} \tag{9}$$

$$\psi_{q'}(\boldsymbol{q}') \triangleq \frac{\partial \psi}{\boldsymbol{q}'}. \tag{10}$$

In relation to (8) and (9), define

$$\overline{\psi}(\boldsymbol{q}', \boldsymbol{q}) \triangleq \begin{bmatrix} \phi(\boldsymbol{q}') \\ \alpha(\boldsymbol{q}') \end{bmatrix} - \begin{bmatrix} 0 \\ \boldsymbol{q} \end{bmatrix} \tag{11}$$

and $\overline{\psi}_{q'}(\boldsymbol{q}') \triangleq \partial\overline{\psi}/\partial\boldsymbol{q}'$. Further note that $\overline{\psi}_{q'} = \psi_{q'}$. We now define the set

$$\boldsymbol{V}' \triangleq \{\boldsymbol{q}' \in \boldsymbol{U}': \quad \det[\psi_{q'}(\boldsymbol{q}')] \neq 0\} \subset \boldsymbol{U}'.$$

We say that the system is in a singular configuration when $\boldsymbol{q}'$ is an element of $\boldsymbol{U}'$ but is not an element of $\boldsymbol{V}'$. It follows that $\boldsymbol{V}'$ is the workspace region in the $\boldsymbol{q}'$ coordinates where the constrained system satisfies the constraints and in addition is not in a singular configuration.

Remark II.2: A useful mechanical system should satisfy the constraints and should not be permanently in a singular configuration. Consequently, $\boldsymbol{V}' \neq \emptyset$ in general. If this is not the case, the system should be mechanically redesigned. Hence, it is reasonable to assume that $\boldsymbol{V}'$ contains nonempty regions which, of course, are not necessarily connected.

We now have the following result.

Lemma II.1: For any given point $\boldsymbol{q}'_\star \in \boldsymbol{V}'$, let $\overline{\psi}(\boldsymbol{q}'_\star, \boldsymbol{q}_\star) = 0$. Then there exist a neighborhood $\mathcal{N}_{q'_\star}$ of $\boldsymbol{q}'_\star$, and a neighborhood $\mathcal{N}_{q_\star}$ of $\boldsymbol{q}_\star$, such that for any $\boldsymbol{q} \in \mathcal{N}_{q_\star}$, there exists a unique $\boldsymbol{q}' \in \mathcal{N}_{q'_\star}$, such that

$$q' = \sigma(\boldsymbol{q}). \tag{12}$$

Furthermore

$$\dot{\boldsymbol{q}}' = \rho(\boldsymbol{q}')\dot{\boldsymbol{q}} \tag{13}$$

where

$$\rho(\boldsymbol{q}') = \psi_{q'}^{-1}(\boldsymbol{q}') \begin{bmatrix} 0_{(n'-n)\times n} \\ I_{n\times n} \end{bmatrix}. \tag{14}$$

Proof of Lemma II.1: For any given point $\boldsymbol{q}'_\star \in \boldsymbol{V}'$ we have by definition $\boldsymbol{q}_\star = \alpha(\boldsymbol{q}'_\star)$, $\overline{\psi}(\boldsymbol{q}'_\star, \boldsymbol{q}_\star) = 0$, and $\det[\overline{\psi}_{q'}(\boldsymbol{q}'_\star, \boldsymbol{q}_\star)] \neq 0$. Therefore, we conclude, using the classical implicit function theorem [59], that in neighborhoods $\mathcal{N}_{q'_\star}$ of $\boldsymbol{q}'_\star$ and $\mathcal{N}_{q_\star}$ of $\boldsymbol{q}_\star$, the equation $\overline{\psi}(\boldsymbol{q}', \boldsymbol{q}) = 0$ determines $\boldsymbol{q}'$ uniquely as a continuously differentiable function of $\boldsymbol{q}$, namely, $\boldsymbol{q}' = \sigma(\boldsymbol{q})$.

Equation (14) follows from taking the derivative of (8), namely

$$\psi_{q'}(q')\dot{\boldsymbol{q}}' = \begin{bmatrix} 0_{(n'-n)\times n} \\ I_{n\times n} \end{bmatrix} \dot{\boldsymbol{q}}$$

and rewriting it as follows:

$$\begin{aligned} \dot{\boldsymbol{q}}' &= \psi_{q'}^{-1}(\boldsymbol{q}') \begin{bmatrix} 0_{(n'-n)\times n} \\ I_{n\times n} \end{bmatrix} \dot{\boldsymbol{q}} \\ &= [\, X(\boldsymbol{q}') \quad \rho(\boldsymbol{q}') \,] \begin{bmatrix} 0_{(n'-n)\times n} \\ I_{n\times n} \end{bmatrix} \dot{\boldsymbol{q}}. \end{aligned}$$

$\square$

We now let $\boldsymbol{W}' \subset \boldsymbol{V}'$ denote the *largest* subset of $\boldsymbol{V}'$ containing $\boldsymbol{q}'_\star$ for which the unique parametrization (12) holds. We denote the corresponding domain of σ by $\boldsymbol{\Omega}$. Hence, we have a diffeomorphism from $\boldsymbol{W}'$ to $\boldsymbol{\Omega}$ as follows: $\boldsymbol{W}' \xrightarrow{\alpha} \boldsymbol{\Omega} \xrightarrow{\sigma} \boldsymbol{W}'$.

Note that the parameterization (12) cannot in general be expressed explicitly in an analytical form. It can only be computed iteratively by numerically solving (11) which, as proved in Lemma II.1, admits a unique solution $\boldsymbol{q}' = \sigma(\boldsymbol{q})$ when $\boldsymbol{q} \in \boldsymbol{\Omega}$. With an estimate of the domain $\boldsymbol{\Omega}$ including its boundaries as will be proposed in a later section, a numerical iterative algorithm, such as Newton–Raphson algorithm, can be set up in such a manner that for a given $\boldsymbol{q}_0 \in \boldsymbol{\Omega}$, a convergent solution $\boldsymbol{q}'_0 = \sigma(\boldsymbol{q}_0) \in \boldsymbol{W}'$ with a given accuracy can be obtained in a finite number of iterations. A detailed study of such an iterative algorithm can be found in [12] and [13].

C. Reduced Model

We now reconsider the constraint (3) which, due to its assumed differentiability properties (Assumption II.1), can be differentiated twice with respect to time and hence we obtain

$$\phi_{q'}(q')\dot{\boldsymbol{q}}' = 0 \tag{15}$$

$$\phi_{q'}(\boldsymbol{q}')\ddot{\boldsymbol{q}}' + \dot{\phi}_{q'}(\boldsymbol{q}', \dot{\boldsymbol{q}}')\dot{\boldsymbol{q}}' = 0. \tag{16}$$

It is a standard result from classical dynamics [26] that the constrained system is completely described by the following algebraic-differential equation obtained from using (2) and (15):

$$D'(\boldsymbol{q}'), \ddot{\boldsymbol{q}}' + C'(\boldsymbol{q}', \dot{\boldsymbol{q}}')\dot{\boldsymbol{q}}' + \boldsymbol{g}'(\boldsymbol{q}') = \phi_{q'}^T(\boldsymbol{q}')\lambda \tag{17}$$

$$\phi_{q'}(\boldsymbol{q}')\dot{\boldsymbol{q}}' = 0 \tag{18}$$

where λ is the vector of Lagrange multipliers and $\phi_{q'}^T\lambda$ represents the constraint generalized force vector. Equivalently, using (16), we obtain

$$\begin{bmatrix} D'(\boldsymbol{q}') & -\phi_{q'}^T(\boldsymbol{q}') \\ \phi_{q'}(\boldsymbol{q}') & 0 \end{bmatrix} \begin{bmatrix} \ddot{\boldsymbol{q}}' \\ \lambda \end{bmatrix} + \begin{bmatrix} C'(\boldsymbol{q}', \dot{\boldsymbol{q}}'), \dot{\boldsymbol{q}}' + \boldsymbol{g}'(\boldsymbol{q}') \\ \dot{\phi}_{q'}(\boldsymbol{q}', \dot{\boldsymbol{q}}')\dot{\boldsymbol{q}}' \end{bmatrix} = \begin{bmatrix} 0 \\ 0 \end{bmatrix}. \tag{19}$$

Since the inertia matrix $D'(\boldsymbol{q}')$ is positive definite, and the constraints (3) are by assumption independent, hence $\phi_{q'}(\boldsymbol{q}')$ is of full $(n' - n)$ rank (refer to Note II.1), it follows that the coefficient matrix of the left side of (20) is nonsingular and that (20) has a unique solution for $\ddot{\boldsymbol{q}}'$ and in particular for λ. Consequently, a complete description of the constrained system in terms of dependent coordinates $\boldsymbol{q}'$ is given by (17) with λ explicitly solved for.

We now consider the virtual work expression δW associated with the dynamics of the constrained system (17), namely

$$\delta W = \delta \boldsymbol{q}'^T \left[D'(\boldsymbol{q}')\ddot{\boldsymbol{q}}' + C'(\boldsymbol{q}', \dot{\boldsymbol{q}}')\dot{\boldsymbol{q}}' + \boldsymbol{g}'(\boldsymbol{q}') - \phi_{q'}^T(\boldsymbol{q}')\lambda \right].$$

It is clear from (17) that $\delta W = 0$ for any set of $\delta \boldsymbol{q}'$. Assuming that $\delta \boldsymbol{q}'$ conform to the instantaneous constraints, then the virtual work of the constraints vanishes, that is, $\delta \boldsymbol{q}'^T \phi_{q'}^T \lambda = 0$, and consequently

$$\delta \boldsymbol{q}'^T \left[D'(\boldsymbol{q}')\ddot{\boldsymbol{q}}' + C'(\boldsymbol{q}', \dot{\boldsymbol{q}}')\dot{\boldsymbol{q}}' + \boldsymbol{g}'(\boldsymbol{q}') \right] = 0. \tag{20}$$

Noting from (13) that $\forall (\boldsymbol{q}', \boldsymbol{q}) \in \boldsymbol{W}' \times \boldsymbol{\Omega}$ we have $\delta \boldsymbol{q}' = \rho(\boldsymbol{q}')\delta \boldsymbol{q}$, and using (20), it follows that

$$\delta \boldsymbol{q}^T \left[\rho(\boldsymbol{q}')^T D'(\boldsymbol{q}')\ddot{\boldsymbol{q}}' + \rho(\boldsymbol{q}')^T C'(\boldsymbol{q}', \dot{\boldsymbol{q}}')\dot{\boldsymbol{q}}' + \rho(\boldsymbol{q}')^T \boldsymbol{g}'(\boldsymbol{q}') \right] = 0.$$

Since the generalized coordinates $\boldsymbol{q}$ are independent, we obtain

$$\rho(\boldsymbol{q}')^T D'(\boldsymbol{q}')\ddot{\boldsymbol{q}}' + \rho(\boldsymbol{q}')^T C'(\boldsymbol{q}', \dot{\boldsymbol{q}}')\dot{\boldsymbol{q}}' + \rho(\boldsymbol{q}')^T \boldsymbol{g}'(\boldsymbol{q}') = 0. \tag{21}$$

Taking the derivative of (13), that is, $\ddot{\boldsymbol{q}}' = \dot{\rho}(\boldsymbol{q}', \dot{\boldsymbol{q}}')\dot{\boldsymbol{q}} + \rho(\boldsymbol{q}')\ddot{\boldsymbol{q}}$, and combining with (21), we obtain the equations of motion of the constrained system in terms of $(\boldsymbol{q}', \boldsymbol{q}) \in \boldsymbol{W}' \times \boldsymbol{\Omega}$ as follows:

$$D(\boldsymbol{q}')\ddot{\boldsymbol{q}} + C(\boldsymbol{q}', \dot{\boldsymbol{q}}')\dot{\boldsymbol{q}} + \boldsymbol{g}(\boldsymbol{q}') = 0 \tag{22}$$

where $\forall\, \boldsymbol{q}' \in \boldsymbol{W}'$

$$D(\boldsymbol{q}') = \rho(\boldsymbol{q}')^T D'(\boldsymbol{q}')\rho(\boldsymbol{q}') \tag{23}$$

$$\begin{aligned} C(\boldsymbol{q}', \dot{\boldsymbol{q}}') =& \rho(\boldsymbol{q}')^T C'(\boldsymbol{q}', \dot{\boldsymbol{q}}')\rho(\boldsymbol{q}') \\ &+ \rho(\boldsymbol{q}')^T D'(\boldsymbol{q}')\dot{\rho}(\boldsymbol{q}', \dot{\boldsymbol{q}}') \end{aligned} \tag{24}$$

$$\boldsymbol{g}(\boldsymbol{q}') = \rho(\boldsymbol{q}')^T \boldsymbol{g}'(\boldsymbol{q}') \tag{25}$$

where $\rho(\boldsymbol{q}')$ is given by (14).

We now present the first main result of the paper in the following theorem the proof of which follows from the previous derivations.

Theorem 1: The equations of motion of the constrained system expressed in terms of independent generalized coordinates $\boldsymbol{q} \in \boldsymbol{\Omega}$, as given in (5) and repeated here for convenience

$$\Sigma: \quad D(\boldsymbol{q})\ddot{\boldsymbol{q}} + C(\boldsymbol{q}, \dot{\boldsymbol{q}})\dot{\boldsymbol{q}} + \boldsymbol{g}(\boldsymbol{q}) = 0 \tag{26}$$

are obtained by combining

$$\begin{cases} D(\boldsymbol{q}')\ddot{\boldsymbol{q}} + C(\boldsymbol{q}', \dot{\boldsymbol{q}}')\dot{\boldsymbol{q}} + \boldsymbol{g}(\boldsymbol{q}') = 0 & (22) \\ \dot{\boldsymbol{q}}' = \rho(\boldsymbol{q}')\dot{\boldsymbol{q}} & (13) \\ \boldsymbol{q}' = \sigma(\boldsymbol{q}) \end{cases} \tag{27}$$

where the existence of $\sigma(\boldsymbol{q})$ is insured by the implicit function theorem. □

The reduced model described above in (27) has two special characteristics which make it different from regular models of open-chain mechanical systems. First, the above reduced model is valid only (locally) in $\boldsymbol{q}$ in a compact set $\boldsymbol{\Omega}$. Second, since the parameterization $\boldsymbol{q}' = \sigma(\boldsymbol{q})$ is implicit, it is an implicit model.

D. Characterization of the Domain of Definition $\boldsymbol{\Omega}$

One can easily be misled to the conclusion that any singularity-free connected domain where the Jacobian (10) is nonsingular throughout, say $\boldsymbol{W}'_c \subset \boldsymbol{W}'$, could be considered as a candidate for the domain $\boldsymbol{\Omega} = \alpha(\boldsymbol{W}'_c)$ in which a diffeomorphism (12) exists throughout. This is the result of the improper extensions of some well known results like the implicit function theorem or Rolle's theorem. It is worthwhile to emphasize that if the Jacobian (10) is nonsingular at a given vector point, then the implicit function theorem will only guarantee a diffeomorphism (12) in a neighborhood of the point with unspecified boundaries. On the other hand, if the Jacobian (10) is nonsingular throughout a compact set, then Rolle's theorem provides a global domain where a diffeomorphism (12) exists throughout a compact set; but this is guaranteed for single variable functions only. The best way to correct the fallacious intuition that Rolle's theorem works for multivariable functions is to study closed-chain mechanisms that can go from one joint configuration to another without passing through singularities [29], [49]. There exist so-called global implicit function theorems [28], [53] as well as a generalization of Rolle's theorem presented in [50], both of which provide explicit boundaries of the domain and extend the traditional implicit function theorem [59] by imposing additional conditions for the existence of a diffeomorphism between two precise sets. Unfortunately these conditions are hard to characterize for a given physical system. In conclusion, it is not generally easy to explicitly characterize the boundaries of the domain $\mathbf{\Omega}$.

On the other hand, if one would be satisfied with a conservative estimate of the boundaries of the domain of $\mathbf{\Omega}$, the approach that exploits Kantorovich theorem [58] gives relatively good results with only modest computational effort. Without getting into too much details (cf. [12]), this approach necessitates certain properties of the function $\psi(\boldsymbol{q}')$ in (9): the latter has to be a polynomial with no monome of degree higher than two. In case these conditions are not satisfied, a remedy would be to rewrite the expression of $\psi(\boldsymbol{q}')$. In fact, note that ψ is obtained from (8), and a small modification of $\boldsymbol{q}$ and $\boldsymbol{q}'$ in this system would transform ψ into the desired form. For example, if we had

$$\underbrace{\begin{bmatrix} x\cos\theta - 1 \\ x\sin\theta - 2y \\ \arccos(y^3 - 3\,x^2\,y) \end{bmatrix}}_{\psi(\boldsymbol{q}')} = \begin{bmatrix} 0 \\ 0 \\ \varphi \end{bmatrix}$$

with

$$\boldsymbol{q}' = \begin{bmatrix} x \\ y \\ \theta \end{bmatrix} \quad \text{and} \quad \boldsymbol{q} = [\varphi]$$

then we modify this system to have

$$\underbrace{\begin{bmatrix} xu - 1 \\ xv - 2y \\ u^2 + v^2 - 1 \\ x^2 - w \\ y^2 - s \\ sy - 3wy \end{bmatrix}}_{\psi(\boldsymbol{q}')} = \begin{bmatrix} 0 \\ 0 \\ 0 \\ 0 \\ 0 \\ r \end{bmatrix}$$

with

$$\boldsymbol{q}' = \begin{bmatrix} x \\ y \\ u \\ v \\ w \\ s \end{bmatrix} \quad \text{and} \quad \boldsymbol{q} = [r].$$

Note that adding equation ($u^2 + v^2 - 1 = 0$) eliminates $\cos\theta$ and $\sin\theta$, while adding ($x^2 - w = 0$) and ($y^2 - s = 0$) "breaks" the monomes of degree higher than two. The change of variables made in this operation is very simple, which implies that the set $\mathbf{\Omega}$ characterized in the new $\boldsymbol{q}$ variable could be easily interpreted in terms of the original $\boldsymbol{q}$ variables.

The function ψ, now polynomial with no monome of degree higher than two, satisfies a rather remarkable property: its Jacobian $\psi_{q'}$ is *globally* Lipschitz in $\Re^{n'}$, that is, $\|\psi_{q'}(\boldsymbol{x}) - \psi_{q'}(\boldsymbol{y})\|_\infty \le c\|\boldsymbol{x} - \boldsymbol{y}\|_\infty$ where $\|\cdot\|_\infty$ is the infinity norm. This property is the result of the fact that each element of the matrix is affine since it is obtained by taking the derivative of a polynomial of degree two. Due to the equivalence of norms in $\Re^{n'}$ [32], [63], the Lipschitz property is valid for all norms; the infinity norm in particular facilitates the computation of the Lipschitz constant c. In fact, the latter is easily obtained [13] from the expression of $\psi_{q'}$ by setting to zero all monome of degree zero, changing the signs $-$ to $+$, replacing all variables by one, summing the elements of each line and taking the maximum of the resulting vector $\boldsymbol{v}$. For example, if we take the Jacobian $\psi_{q'}$ resulting from the function of the above example, we obtain

$$\psi_{q'} = \begin{bmatrix} u & 0 & x & 0 & 0 & 0 \\ v & 0 & 0 & x & 0 & 0 \\ 0 & 0 & 2u & 2v & 0 & 0 \\ 2x & 0 & 0 & 0 & -1 & 0 \\ 0 & 2y & 0 & 0 & 0 & -1 \\ 0 & s - 3w & 0 & 0 & -3y & y \end{bmatrix}$$

$$\boldsymbol{v} = \begin{bmatrix} 1+1 \\ 1+1 \\ 2+2 \\ 2 \\ 2 \\ (1+3)+3+1 \end{bmatrix}; \qquad c = 8.$$

Kantorovich theorem [58], which can be exploited in our case thanks to the Lipschitz property established above, plays a central role in the Theorem 2 that follows. Due to limited space, the reader is referred to [11]–[13] for detailed proof of Theorem 2.

Theorem 2: The explicit radius r of the domain $\mathbf{\Omega}$ centered at $\boldsymbol{q}_0 = \alpha(\boldsymbol{q}_0')$, that is

$$\mathbf{\Omega} = \{\boldsymbol{q}\colon \|\boldsymbol{q} - \boldsymbol{q}_0\|_\infty < r\}$$

is given by the following expression:

$$r = \frac{1}{2} \cdot \frac{1}{\|\psi_{q'}^{-1}(\boldsymbol{q}_0') \cdot \mathrm{diag}(\boldsymbol{v})\|_\infty} \cdot \frac{1}{\|\psi_{q'}^{-1}(\boldsymbol{q}_0') \cdot \mathrm{diag}([0\ \cdots\ 0\ \underbrace{1\ \cdots\ 1}_{n\times}])\|_\infty}$$

where $\mathrm{diag}(\cdot)$ is a diagonal matrix with the given argument and $\boldsymbol{v}$ is the vector constructed similar to the method of example (28).

III. PD-Based Control Strategies

To investigate the applicability of PD-based control strategies for closed-chain mechanisms with guaranteed stability properties, we first consider two important issues with respect to the reduced model (27), namely, the skew symmetry property, and the computation of the gravity vector.

Lemma III.1—Skew Symmetry: The matrix $\dot{D} - 2C$ is skew symmetric.

Proof of Lemma III.1: Using (23) and (24), we have

$$\begin{aligned} \dot{D} - 2C &= \dot{\rho}^T D' \rho + \rho^T D' \dot{\rho} + \rho^T \dot{D}' \rho - 2\rho^T C' \rho - 2\rho^T D' \dot{\rho} \\ &= \Delta + \rho^T \left[\dot{D}' - 2C'\right] \rho \end{aligned}$$

where $\Delta = [\dot{\rho}^T D' \rho + \rho^T D' \dot{\rho} - 2\rho^T D' \dot{\rho}]$. First, note that $\Delta + \Delta^T = 0$ and hence Δ is skew symmetric. Second, note that for the free system, the matrix $\dot{D}' - 2C'$ is skew symmetric.

Since $T^T[\dot{D}' - 2C']T$ is also skew symmetric for any matrix T with appropriate dimension, in particular for $T = \rho$, it follows that $\rho^T[\dot{D}' - 2C']\rho$ is skew symmetric. Hence $\dot{D} - 2C$ is skew symmetric since it is the sum of two skew symmetric matrices.☐

The computation of the gravity vector $\boldsymbol{g}(\boldsymbol{q})$ involves essentially the computation of the parameterization $\boldsymbol{q}' = \sigma(\boldsymbol{q})$, the computation of expression (14), and the substitution of both in (25). The parameterization $\boldsymbol{q}' = \sigma(\boldsymbol{q})$ is in general impossible to compute explicitly, but a simple algorithm could be formulated to numerically compute it. In fact, it was discussed earlier that a numerical iterative algorithm, such as Newton–Raphson algorithm, can be set up in such a manner that for a given $\boldsymbol{q}_0 \in \boldsymbol{\Omega}$, a convergent solution $\boldsymbol{q}_0' = \sigma(\boldsymbol{q}_0) \in \boldsymbol{W}'$ with a given accuracy can be obtained in a finite number of iterations [12], [13]. The gravity vector is consequently computed using the expressions (14) and (25). In conclusion, the computation of the gravity vector is numerically well posed.

Let us now consider a set-point (regulation) problem in which it is required that the vector $\boldsymbol{q}$ reach a constant desired value $\overline{\boldsymbol{q}}_d \in \boldsymbol{\Omega}$. Define $\tilde{\boldsymbol{q}} \triangleq \overline{\boldsymbol{q}}_d - \boldsymbol{q}$, and $\mathcal{B} \triangleq \{(\tilde{\boldsymbol{q}}, \dot{\boldsymbol{q}})\colon \boldsymbol{q}, \overline{\boldsymbol{q}}_d \in \boldsymbol{\Omega}\}$. We consider a PD-based control strategy for general closed-chain mechanisms that guarantees Lyapunov asymptotic stability.

A. PD Plus Simple Gravity Compensation

We consider the most general case of closed-chain structures in which the parametrization $\boldsymbol{q}' = \sigma(\boldsymbol{q})$, and hence the gravity vector expression $\boldsymbol{g}(\boldsymbol{q}) = \rho^T(\sigma(\boldsymbol{q}))\boldsymbol{g}'(\sigma(\boldsymbol{q}))$, are implicit expressions. We propose a control law which consists of compensating for the gravity at the desired position only, an idea presented first in [4], later in [37], and then in [61] for serial link (open-chain) manipulators. The control law is given by

$$u = K_p\tilde{\boldsymbol{q}} - K_v\dot{\boldsymbol{q}} + \boldsymbol{g}_c(\overline{\boldsymbol{q}}_d). \tag{28}$$

Note that the term[2] $\boldsymbol{g}_c(\overline{\boldsymbol{q}}_d) = \rho^T(\sigma_c(\overline{\boldsymbol{q}}_d))\boldsymbol{g}'(\sigma_c(\overline{\boldsymbol{q}}_d))$ in (28) is *constant* and can therefore be numerically computed *off-line*. In addition, since the computation is performed off-line, $\boldsymbol{g}_c(\overline{\boldsymbol{q}}_d)$ can be computed to any degree of accuracy. Hence, it is safe to write $\boldsymbol{g}(\overline{\boldsymbol{q}}_d) = \boldsymbol{g}_c(\overline{\boldsymbol{q}}_d) = \rho^T(\sigma(\overline{\boldsymbol{q}}_d))\boldsymbol{g}'(\sigma(\overline{\boldsymbol{q}}_d))$. Combining the equations of motion (27) and the control law (28) and using $\boldsymbol{g}_c(\overline{\boldsymbol{q}}_d) = \boldsymbol{g}(\overline{\boldsymbol{q}}_d)$, we obtain

$$D(\boldsymbol{q})\ddot{\boldsymbol{q}} + C(\boldsymbol{q}, \dot{\boldsymbol{q}})\dot{\boldsymbol{q}} + \boldsymbol{g}(\boldsymbol{q}) = K_p\tilde{\boldsymbol{q}} - K_v\dot{\boldsymbol{q}} + \boldsymbol{g}(\overline{\boldsymbol{q}}_d). \tag{29}$$

It can be easily seen that ($\tilde{\boldsymbol{q}} = 0$, $\dot{\boldsymbol{q}} = 0$) is an equilibrium. We now consider the following function:

$$\begin{aligned}\mathcal{V}(\tilde{\boldsymbol{q}}, \dot{\boldsymbol{q}}) = &\tfrac{1}{2}\dot{\boldsymbol{q}}^T D(q)\dot{\boldsymbol{q}} + V(\boldsymbol{q}) - V(\overline{\boldsymbol{q}}_d)\\ &+ \tilde{\boldsymbol{q}}^T\boldsymbol{g}(\boldsymbol{q}_d) + \tfrac{1}{2}\tilde{\boldsymbol{q}}^T K_p\tilde{\boldsymbol{q}}\end{aligned}$$

where $V(\boldsymbol{q})$ is the potential energy of the plant (27) so that $\partial V/\partial\boldsymbol{q} = \boldsymbol{g}(\boldsymbol{q})$. Note that $\mathcal{V}(\tilde{\boldsymbol{q}}, \dot{\boldsymbol{q}})$ is a locally positive definite function, hence a suitable Lyapunov function candidate to prove asymptotic stability, if

$$\frac{\partial^2}{\partial\boldsymbol{q}^2}\left[V(\boldsymbol{q}) - V(\overline{\boldsymbol{q}}_d) + \tilde{\boldsymbol{q}}^T\boldsymbol{g}(\boldsymbol{q}_d) + \frac{1}{2}\tilde{\boldsymbol{q}}^T K_p\tilde{\boldsymbol{q}}\right] = \partial\boldsymbol{g}/\partial\boldsymbol{q} + K_p$$

is positive definite, insuring that the equilibrium $\tilde{\boldsymbol{q}} = 0$ and $\dot{\boldsymbol{q}} = 0$ is unique $\forall\,(\tilde{\boldsymbol{q}}, \dot{\boldsymbol{q}}) \in \mathcal{B}$.

[2]The subscript "c" emphasizes that the quantity in question is computed numerically.

We now present the second main result in this paper.

Theorem 3: Define the set $\mathcal{B}_2 \triangleq \{(\tilde{\boldsymbol{q}}, \dot{\boldsymbol{q}})\colon \mathcal{V}(\tilde{\boldsymbol{q}}, \dot{\boldsymbol{q}}) \le c\}$ where c is the largest positive real number such that $\mathcal{B}_2 \subset \mathcal{B}$. Let the initial conditions $(\tilde{\boldsymbol{q}}_0, \dot{\boldsymbol{q}}_0) \in \mathcal{B}_2$, and let $\|\partial\boldsymbol{g}(\boldsymbol{q})/\partial\boldsymbol{q}\| \le \beta$ in $\mathcal{B}_2$ where β is a positive constant. Choose $k_{pi} > \beta$, $i = 1, 2, \cdots, n$, where k_{pi} are the diagonal elements of K_p. Then the equilibrium $\tilde{\boldsymbol{q}} = 0$ and $\dot{\boldsymbol{q}} = 0$ of the reduced model (27) with the control law (28) is (locally) asymptotically stable and $\boldsymbol{q} \longrightarrow \overline{\boldsymbol{q}}_d$, $\dot{\boldsymbol{q}} \longrightarrow 0$, as $t \longrightarrow \infty$.

Proof of Theorem 3: Note that the existence of the constant β is insured by the continuity of the gravity vector $\boldsymbol{g}$ since the set $\boldsymbol{\Omega}$, hence $\mathcal{B}_2$, is compact. Furthermore, it can easily be shown that if $k_{pi} > \beta$, $i = 1, 2, \cdots, n$, then $\partial\boldsymbol{g}/\partial\boldsymbol{q} + K_p$ is positive definite insuring, as discussed above, that $\mathcal{V}(\tilde{\boldsymbol{q}}, \dot{\boldsymbol{q}})$ is a Lyapunov function candidate. The time derivative of $\mathcal{V}$ along the solution trajectories of the control system (29) is given by

$$\begin{aligned}\dot{\mathcal{V}} &= \dot{\boldsymbol{q}}^T\{D\ddot{\boldsymbol{q}}\} + \tfrac{1}{2}\dot{\boldsymbol{q}}^T\dot{D}\dot{\boldsymbol{q}} + \boldsymbol{g}(\boldsymbol{q})\dot{\boldsymbol{q}} - \dot{\boldsymbol{q}}^T\boldsymbol{g}(\boldsymbol{q}_d) - \dot{\boldsymbol{q}}^T K_p\tilde{\boldsymbol{q}}\\ &= -\dot{\boldsymbol{q}}^T K_v\dot{\boldsymbol{q}} \le 0.\end{aligned}$$

Note that we substituted (29) and used the skew symmetry property of $\dot{D} - 2C$ which we established earlier in Lemma III.1. We therefore conclude that the equilibrium $\tilde{\boldsymbol{q}} = 0$ and $\dot{\boldsymbol{q}} = 0$ is locally stable. It is now a standard procedure to invoke LaSalle's theorem to conclude (local) asymptotic stability. ☐

Remark III.1: For some closed-chain structures, it may be possible to express the parametrization $\boldsymbol{q}' = \sigma(\boldsymbol{q})$ explicitly in an analytical form. Consequently, the gravity vector $\boldsymbol{g}(\boldsymbol{q}) = \rho^T(\sigma(\boldsymbol{q}))\boldsymbol{g}'(\sigma(\boldsymbol{q}))$ will also be expressed explicitly. Furthermore, a domain $\boldsymbol{\Omega}$ could be directly obtained without reference to the method discussed in Theorem 2. It follows that all the control laws for open-chain mechanisms could also be applied in this case with the only restriction that the guaranteed (Lyapunov) stability conclusions will be local. For example, consider the following PD plus full gravity compensation control law

$$u = K_p\tilde{\boldsymbol{q}} - K_v\dot{\boldsymbol{q}} + \boldsymbol{g}(\boldsymbol{q}) \tag{30}$$

where K_p and K_v are diagonal positive definite constant matrices. The control law (30) along with the equations of motion (27) guarantee local asymptotic stability for set point control (see [20] for details).

IV. An Experimental Case Study

A. The Rice Planar Delta Robot (RPDR)

The RPDR was designed and built at Rice University as a test-bed to perform experiments on closed-chain mechanisms (see Fig. 3). The link configuration is shown in Fig. 4. It has four links connected through revolute joints. Two of the links (Links 1 and 2) are actuated with dc motors while the other two links (Links 3 and 4) are passive. It can be seen that the RPDR has two dofs. Thus, the number of inputs are selected to match the number of degrees of freedom. Even though we will show that explicit equations of motion can be obtained for this system, it can still be used to illustrate the modeling and control ideas presented in this paper for more general closed-chain mechanisms. Furthermore, the explicit equations of motion will enable us to

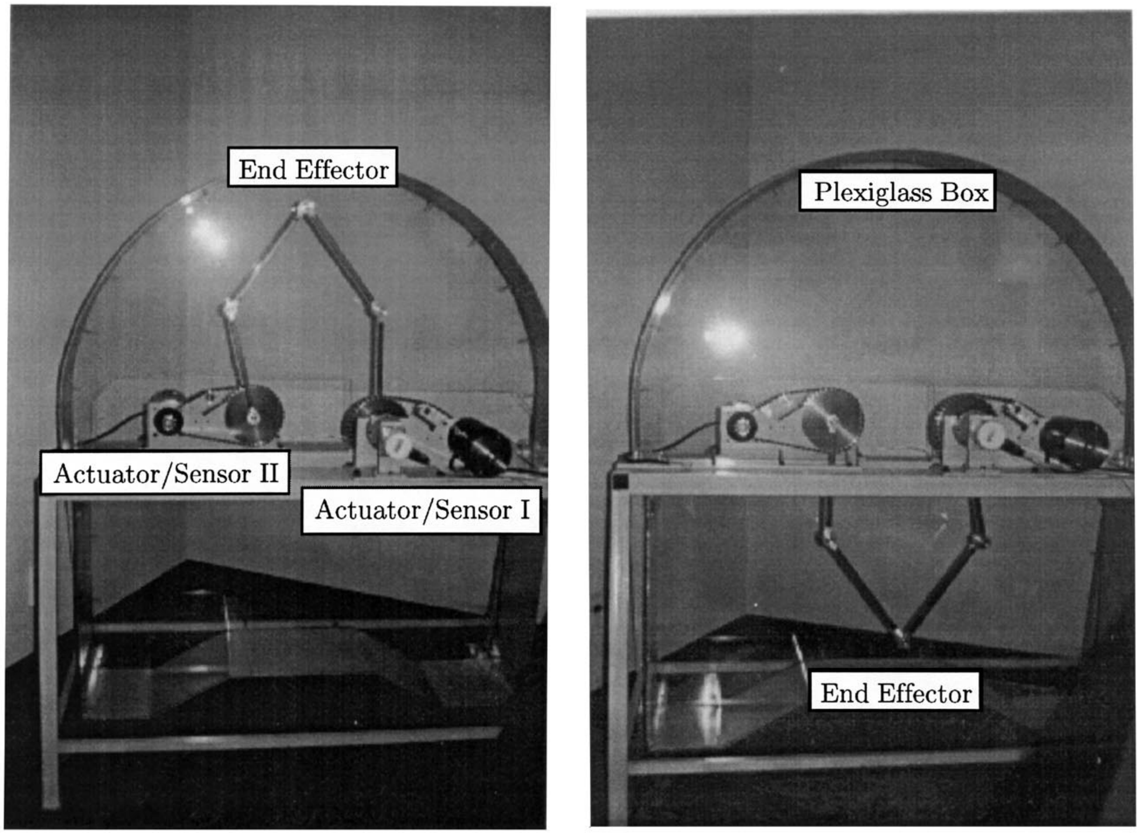

(a) Upward Position (b) Downward Position

Fig. 3. Rice planar delta robot (RPDR).

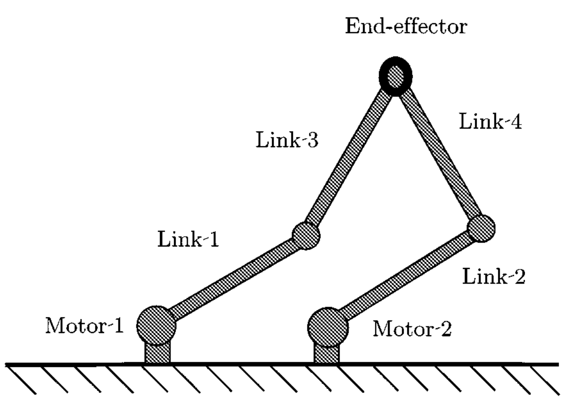

Fig. 4. Link and joint configuration of the RPDR

completely characterize the domain $\mathbf{\Omega}$ and hence compare with the results obtained by using Theorem 2.

We next derive the equations of motion for the RPDR using the formulation derived earlier in the paper. The first step in deriving the equations of motion is selecting the "free system." In our free system, the robot is virtually cut open at the end-effector, resulting in two serial robots each having two dofs (see Fig. 5). As defined in the figure, m_i, c_i, and a_i are, respectively, the mass, distance to the center of mass, and length of link i. The inertia of link i about the line through the center of mass parallel to the axis of rotation is denoted by I_i. The parameters corresponding to Links 1 and 3 are defined similar to the parameters of Links 2 and 4 even though they are not shown in the figure. Thus the constraint equations are due to point E being coincident with point F and are given by as shown in (31) at the bottom of the next page, where $\boldsymbol{q}' = [q_1 \quad q_2 \quad q_3 \quad q_4]^T$ is the generalized coordinate vector of the free system. Note that since the actuated joints are Joints 1 and 2 for the RPDR, we choose the generalized coordinate vector of the constrained system to be $\boldsymbol{q} = [q_1 \quad q_2]^T$. Our next objective will be to derive expressions for each of the terms appearing in (27) for the RPDR to obtain the equations of motion. We begin with the parameterization $\alpha(\boldsymbol{q}') = \boldsymbol{q}$, which is given by

$$\alpha(\boldsymbol{q}') = \begin{bmatrix} 1 & 0 & 0 & 0 \\ 0 & 1 & 0 & 0 \end{bmatrix} \boldsymbol{q}' = \boldsymbol{q}. \tag{32}$$

Now by combining (31) and (32) and differentiating with respect to $\boldsymbol{q}'$, we obtain (33) as shown at the bottom of the next page, for $\psi_{\boldsymbol{q}'}(\boldsymbol{q}')$ where, $\psi_{q'}(1, 1) = -a_1 \sin(q_1) - a_3 \sin(q_1 + q_3)$, $\psi_{q'}(1, 2) = a_2 \sin(q_2) + a_4 \sin(q_2 + q_4)$, $\psi_{q'}(2, 1) = a_1 \cos(q_1) + a_3 \cos(q_1 + q_3)$, and $\psi_{q'}(2, 2) = -a_2 \cos(q_2) - a_4 \cos(q_2 + q_4)$. Now from (14) we have the following expression for $\rho(\boldsymbol{q}')$:

$$\rho(\boldsymbol{q}') = \psi_{\boldsymbol{q}'}^{-1}(\boldsymbol{q}') \begin{bmatrix} 0 & 0 \\ 0 & 0 \\ 1 & 0 \\ 0 & 1 \end{bmatrix}. \tag{34}$$

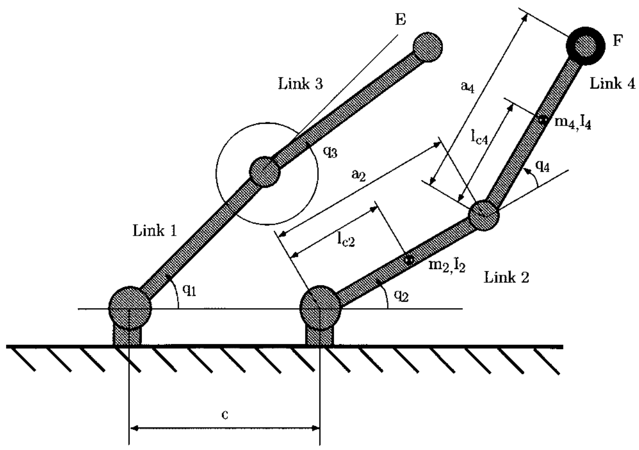

Fig. 5. The "free system."

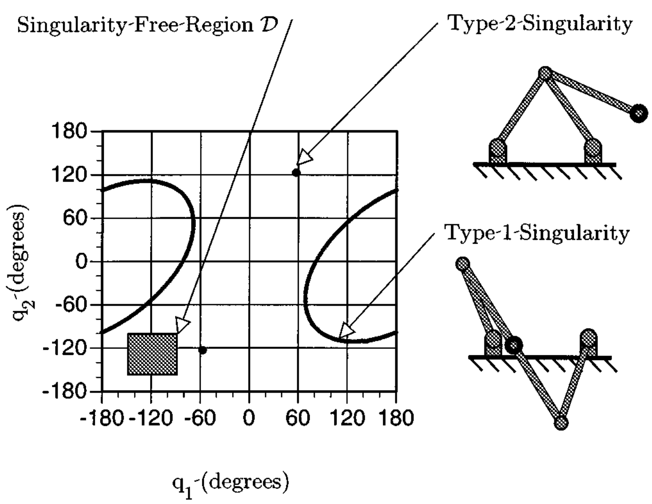

Fig. 6. Singular configurations of the RPDR and the region $\mathcal{D}$.

We next premultiply (34) with $\psi_{\boldsymbol{q}'}(\boldsymbol{q}')$ and taking the time derivative

$$\dot{\rho}(\boldsymbol{q}', \dot{\boldsymbol{q}}') = -\psi_{\boldsymbol{q}'}^{-1}(\boldsymbol{q}')\dot{\psi}_{\boldsymbol{q}'}(\boldsymbol{q}', \dot{\boldsymbol{q}}')\rho(\boldsymbol{q}') \tag{35}$$

where $\dot{\psi}_{\boldsymbol{q}'}(\boldsymbol{q}', \dot{\boldsymbol{q}}')$ can be obtained by differentiating (33) with respect to time. Next we will derive expressions for $D'(\boldsymbol{q}')$, $C'(\boldsymbol{q}', \dot{\boldsymbol{q}}')$, and $\boldsymbol{g}'(\boldsymbol{q}')$ that appear in (23)–(25). The following expressions were derived using the Lagrangian method:

$$D'(\boldsymbol{q}') = \begin{bmatrix} d_{1,1} & 0 & d_{1,3} & 0 \\ 0 & d_{2,2} & 0 & d_{2,4} \\ d_{3,1} & 0 & d_{3,3} & 0 \\ 0 & d_{4,2} & 0 & d_{4,4} \end{bmatrix}, \tag{36}$$

where

$$\begin{aligned}
d_{1,1} &= m_1 l_{c1}^2 + m_3\left(a_1^2 + l_{c3}^2 + 2a_1 l_{c3}\cos(q_3)\right) + I_1 + I_3,\\
d_{1,3} &= m_3\left(l_{c3}^2 + a_1 l_{c3}\cos(q_3)\right) + I_3,\\
d_{2,2} &= m_2 l_{c2}^2 + m_4\left(a_2^2 + l_{c4}^2 + 2a_2 l_{c4}\cos(q_4)\right) + I_2 + I_4,\\
d_{2,4} &= m_4\left(l_{c4}^2 + a_2 l_{c4}\cos(q_4)\right) + I_4,\\
d_{3,1} &= d_{1,3},\\
d_{3,3} &= m_3 l_{c3}^2 + I_3,\\
d_{4,2} &= d_{2,4},\\
d_{4,4} &= m_4 l_{c4}^2 + I_4
\end{aligned}$$

$$C'(\boldsymbol{q}', \dot{\boldsymbol{q}}') = \begin{bmatrix} h_1\dot{q}_3 & 0 & h_1(\dot{q}_1 + \dot{q}_3) & 0 \\ 0 & h_2\dot{q}_4 & 0 & h_2(\dot{q}_2 + \dot{q}_4) \\ -h_1\dot{q}_1 & 0 & 0 & 0 \\ 0 & -h_2\dot{q}_2 & 0 & 0 \end{bmatrix} \tag{37}$$

where $h_1 = -m_3 a_1 l_{c3}\sin(q_3)$, $h_2 = -m_4 a_2 l_{c4}\sin(q_4)$, and

$$\boldsymbol{g}'(\boldsymbol{q}') = \begin{bmatrix} (m_1 l_{c1} + m_3 a_1)\cos(q_1) + m_3 l_{c3}\cos(q_1 + q_3) \\ (m_2 l_{c2} + m_4 a_2)\cos(q_2) + m_4 l_{c4}\cos(q_2 + q_4) \\ m_3 l_{c3}\cos(q_1 + q_3) \\ m_4 l_{c4}\cos(q_2 + q_4) \end{bmatrix} g \tag{38}$$

where $g = 9.81$ m/s^2 is the gravitational acceleration constant. At this point we have derived the equations of motion of the RPDR in terms of $\boldsymbol{q}'$. The only remaining task is the derivation of the parameterization $\boldsymbol{q}' = \sigma(\boldsymbol{q})$. In general, it is not possible to derive an analytic expression for $\sigma(\boldsymbol{q})$, and it must be computed

$$\phi(\boldsymbol{q}') = \begin{bmatrix} a_1\cos(q_1) + a_3\cos(q_1 + q_3) - c - a_2\cos(q_2) - a_4\cos(q_2 + q_4) \\ a_1\sin(q_1) + a_3\sin(q_1 + q_3) - a_2\sin(q_2) - a_4\sin(q_2 + q_4) \end{bmatrix} = \mathbf{0} \tag{31}$$

$$\psi_{\boldsymbol{q}'}(\boldsymbol{q}') = \begin{bmatrix} \psi_{q'}(1,1) & \psi_{q'}(1,2) & -a_3\sin(q_1 + q_3) & a_4\sin(q_2 + q_4) \\ \psi_{q'}(2,1) & \psi_{q'}(2,2) & a_3\cos(q_1 + q_3) & -a_4\cos(q_2 + q_4) \\ 1 & 0 & 0 & 0 \\ 0 & 1 & 0 & 0 \end{bmatrix} \tag{33}$$

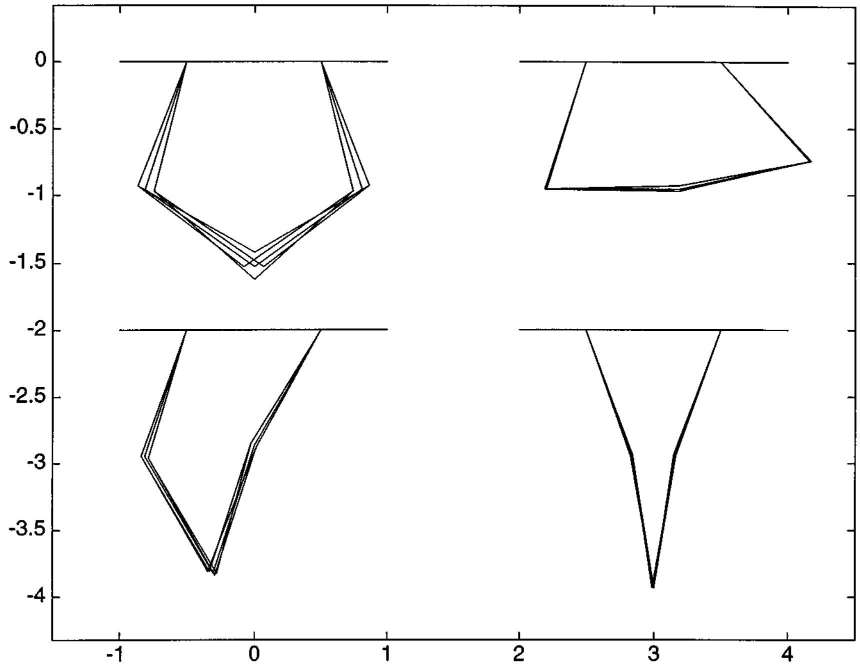

Fig. 7. Boundaries of the domain $\mathbf{\Omega}$ for the RPDR using Theorem 2.

TABLE I
DATA CORRESPONDING TO FIG. 7

$\mathbf{q}_0$	Radius r of $\mathbf{\Omega}$ [From Theorem ??]
$(-108°, 72°)$	3.5°
$(-108°, 48°)$	0.13°
$(-108°, 120°)$	1.7°
$(-70°, 110°)$	0.31°

TABLE II
KINEMATIC LINK PARAMETERS OF THE RPDR MANIPULATOR

Link i	m_i (kg)	a_i (m)	l_{ci} (m)	I_i (kg m^2)
1	0.2451	0.2794	0.1466	2.779×10^{-3}
2	0.2352	0.2794	0.141	2.607×10^{-3}
3	0.2611	0.3048	0.1581	3.476×10^{-3}
4	0.2611	0.3048	0.1467	3.476×10^{-3}

using numerical methods. For the RPDR however, it is possible to solve (31) to obtain the following:

$$
\begin{aligned}
q_4 = &\tan^{-1}\left[\frac{B(q_1, q_2)}{A(q_1, q_2)}\right] \\
&+ \tan^{-1}\left[\frac{\pm\sqrt{A(q_1, q_2)^2 + B(q_1, q_2)^2 - C(q_1, q_2)^2}}{C(q_1, q_2)}\right] \\
&- q_2
\end{aligned}
\tag{39}
$$

where

$$
\begin{aligned}
A(q_1, q_2) &= 2a_4\lambda(q_1, q_2) \\
B(q_1, q_2) &= 2a_4\mu(q_1, q_2)
\end{aligned}
$$

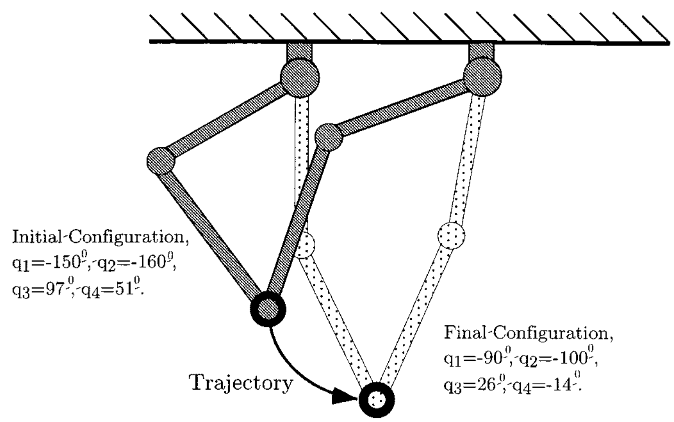

Fig. 8. Point-to-point trajectory.

and

$$C(q_1, q_2) = a_3^2 - a_4^2 - \lambda(q_1, q_2)^2 - \mu(q_1, q_2)^2$$

and

$$
\begin{aligned}
\lambda(q_1, q_2) &= a_2 \cos(q_2) - a_1 \cos(q_1) + c \\
\mu(q_1, q_2) &= a_2 \sin(q_2) - a_1 \sin(q_1).
\end{aligned}
$$

Finally

$$q_3 = \tan^{-1}\left[\frac{\mu(q_1, q_2) + a_4 \sin(q_2 + q_4)}{\lambda(q_1, q_2) + a_4 \cos(q_2 + q_4)}\right] - q_1. \tag{40}$$

Hence, (39) and (40) combined represent the parameterization $\boldsymbol{q}' = \sigma(\boldsymbol{q})$. This completes the derivation of the equations of motion of the RPDR In summary, the equations of motion of the RPDR are given by (27) where $D'(\boldsymbol{q}')$, $C'(\boldsymbol{q}', \dot{\boldsymbol{q}}')$, $\boldsymbol{g}'(\boldsymbol{q}')$,

$\dot{\rho}(\boldsymbol{q}', \dot{\boldsymbol{q}}')$, $\rho(\boldsymbol{q}')$, and $\sigma(\boldsymbol{q})$ are defined in (36)–(38), (35), (34), and (39) plus (40), respectively.

We next characterize a compact domain, a subset of $\boldsymbol{\Omega}$, where the parameterization $\sigma(\boldsymbol{q})$ exists. It turns out that for the RPDR, if we select a simply connected region $\mathcal{D} \subset \Omega$ that is free of singularities, the parameterization $\sigma(\boldsymbol{q})$ will exist in that region. As discussed earlier, this is of course not the case for more general complex systems. Therefore, our first objective was to characterize the singular points of the RPDR from (33), we see that $\det[\psi_{\boldsymbol{q}'}(\boldsymbol{q}')] = \sin(q_1+q_3-q_2-q_4)$. Consequently, the singular points of the RPDR are those for which $(q_1+q_3-q_2-q_4) = n\pi$, for $n = 0, \pm 1, \pm 2, \cdots$. By substituting these into the constraint equations (31), we were able to solve for all of the singular points of the RPDR These are plotted in Fig. 6 which shows the entire workspace of the RPDR (corresponding to the range -180° to 180° for Joints 1 and 2). We considered two cases corresponding to n being even and n being odd. The two cases led to two types of singularities. There are infinitely many singularities of the first type which occur when n is odd. The second type occurs when n is even and the robot loses control of Links 3 and 4 in these configurations. There are two singularities of this type for the RPDR as shown in Fig. 6. For our experiments we chose the singularity free region $\mathcal{D}$ where $-150^\circ \le q_1 \le -90^\circ$ and $-160^\circ \le q_2 \le -100^\circ$.

The application of the result of Theorem 2 to the RPDR is illustrated in Fig. 7: For four different centers $\boldsymbol{q}_0$, the extreme (i.e., boundary) configurations of the robot in the domain $\boldsymbol{\Omega}$ are shown. Table I contains this information in quatitative form.

This example shows that the domain $\boldsymbol{\Omega}$ is very small near singularities. This example, in which comparison with Fig. 6 is possible, also shows that radius r of the domain $\boldsymbol{\Omega}$ computed using Theorem 2 is conservative. Nevertheless, for more complicated systems a detailed analysis like the one given in Fig. 6 will not be feasible, in which case Theorem 2 is the best method available. Most importantly, explicit characterization of a domain $\boldsymbol{\Omega}$, no matter how small, is a prerequisite for performing stability analysis. The latter is not meaningful in an ϵ-neighborhood domain provided by the implicit function theorem.

B. *Experimental PD Control Study*

The RPDR is controlled with an IBM PC to which it is interfaced through a DSP board made by dSPACE [14]. Position feedback of Links 1 and 2 are provided with optical encoders. Velocity feedback is provided by differentiating the position and filtering with a low-pass filter implemented in software. The dSPACE board computes the control law in real time based on the position/velocity feedback and outputs the desired torque at the motors.

The link parameters were calculated and verified by measurement. These are presented in Table II. In addition to the inertia represented in $D(\boldsymbol{q})$, there is a constant inertia due to the motors and the transmission on Joints 1 and 2. These constant inertias were measured to be 3.3263×10^{-3} kg m^2. The distance between the axes of Joints 1 and 2 was measured to be $c = 0.3048$ m.

1) Experimental Results and Simulations—Point to Point Motion: For our experiment, we chose the point to point trajectory shown in Fig. 8 which is within the singularity free region $\mathcal{D}$. The initial configuration is given by $q_1 = -150^\circ$ and $q_2 = -160^\circ$ while the final configuration is given by $q_1 = -90^\circ$ and $q_2 = -100^\circ$. Our next objective was to compute the parameters of the PD with simple gravity compensation control law (28), namely

$$\boldsymbol{u} = \boldsymbol{g}(\boldsymbol{q}^d) + K_P(\boldsymbol{q}^d - \boldsymbol{q}) - K_V\dot{\boldsymbol{q}}.$$

Based on the identified system parameters, we computed the gravity vector at the desired configuration $\boldsymbol{g}(\boldsymbol{q}^d)$ off-line. In order to account for the frictional effects, we estimated Coulomb friction at the desired configuration and added that to $\boldsymbol{g}(\boldsymbol{q}^d)$. Since the effect of viscous friction is to increase K_V, there was no need to account for it. We selected K_P to be diagonal with each element equal to 11 N-m/rad which was sufficient to satisfy the requirements of Theorem 3 for this experiment. The matrix K_V was also selected diagonal with the first element 0.65 and the second element 0.6 N-m-s/rad. The values of the elements of K_V were selected by trial and error to make the system close to critically damped.

In order to compare the experimental results with the theoretical predictions, we performed a simulation. During the simulation we integrated the equations of motion of the RPDR, combined with the control law (28), to generate the solution trajectories. We used the Runge–Kutta algorithm to perform the integration in Matlab. For the simulation, we had the same initial configuration and final desired configuration that was used for the experiments. The simulation and experimental results are presented in Fig. 9. The dashed curves correspond to the simulation results while the solid curves correspond to the experimental results. It can be seen that the experimental and simulation results match well. The slight deviations can be attributed to inexact modeling of friction and other unmodeled dynamics in the system. Furthermore, it can be seen that the robot achieved the desired goal within approximately 0.3 s. It can be seen that the experimental results confirmed the theoretical predictions.

2) Experimental Results and Simulations—Repetitive Point to Point Motion: In some industrial applications, parallel robots are used to perform rapid pick and place routines. In a pick and place routine, a robot moves to one point, picks up an object, carries it to another point, and places the object at that point. In this section we present experimental and simulation results of the RPDR Performing rapid pick and place type motions.

The RPDR was programmed to move repetitively between the initial configuration of Fig. 8 (say $\boldsymbol{q}^i$) and the final configuration (say $\boldsymbol{q}^f$). The algorithm performs the following routine.

1) Implement control law (28) with $\boldsymbol{q}^d = \boldsymbol{q}^f$.
2) After steady state is achieved wait 2.5 s with the control law unchanged.
3) Implement control law (28) with $\boldsymbol{q}^d = \boldsymbol{q}^i$.
4) After steady state is achieved wait 2.5 s with the control law unchanged.
5) Go to Step 1.

As in the point to point motion experiment of Section IV-B1, we compensated for Coulomb friction at the desired configuration. The matrices K_P and K_V were also selected to be the same as in the previous experiment. A simulation was also performed using

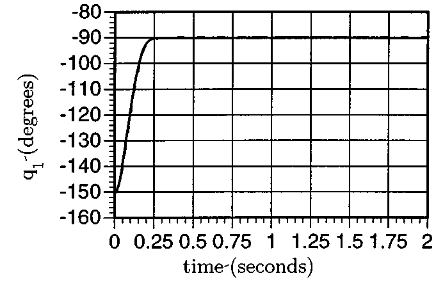

(a) Trajectory Profile of Joint 1

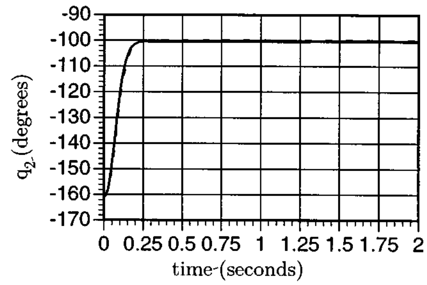

(b) Trajectory Profile of Joint 2

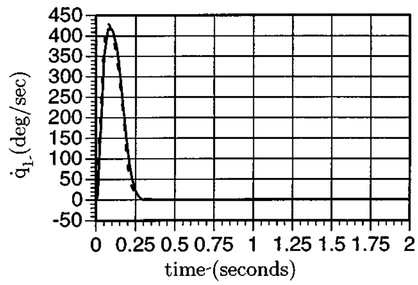

(c) Velocity Profile of Joint 1

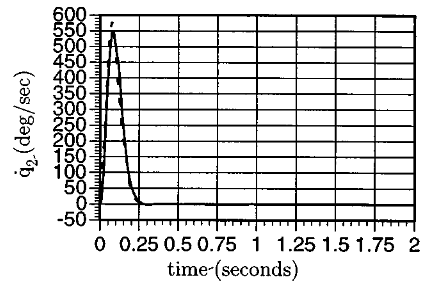

(d) Velocity Profile of Joint 2

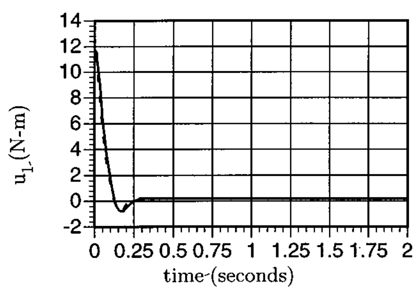

(e) Torque Profile of Joint 1

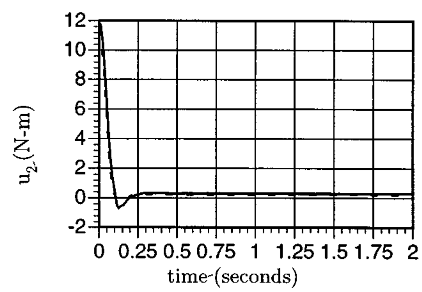

(f) Torque Profile of Joint 2

Fig. 9. Point to point motion: simulation (dashed) and experimental (solid) results: (a) trajectory profile of Joint 1, (b) trajectory profile of Joint 2, (c) velocity profile of Joint 1, (d) velocity profile of Joint 2, (e) torque profile of Joint 1, and (f) torque profile of Joint 2.

the model developed in previous sections. The experimental results and the simulation results are presented in Fig. 10. As in the previous case, the dashed curves correspond to the simulation results while the solid curves correspond to the experimental results. The results show that the robot completed the motion in under 0.3 s and achieved the desired configuration within reasonable tolerances. The simulation and the experimental results seem to agree quite well.

V. Conclusion

In this paper, we developed a procedure to derive the equations of motion of general closed-chain mechanisms. We presented a detailed process to obtain reduced models described in terms of independent generalized coordinates. We showed that the obtained model has two very special properties which make it different from models of open-chain mechanisms. The first property is that the model is defined locally in the generalized coordinates. This is due to the use of the implicit function theorem in the development of the reduced model which can only guarantee the existence of the solution of a zero of a function in some neighborhood (small local domain with unspecified boundaries). We therefore used results from Kantorovich theorem to characterize the domain of validity of the model in which the mechanism satisfies the constraints and is not in a singular configuration. The second property of the reduced model is that it is implicit in the sense that some expressions in the equations of motion are not expressed explicitly because of the use of the implicit function theorem in its development.

The local nature of the reduced model implies that control results can at best guarantee local stability properties. Furthermore, the implicit nature of the model could be a source of difficulty when implementing model-based control laws. The reason is that the implicit terms in the model need to be computed (i.e.,

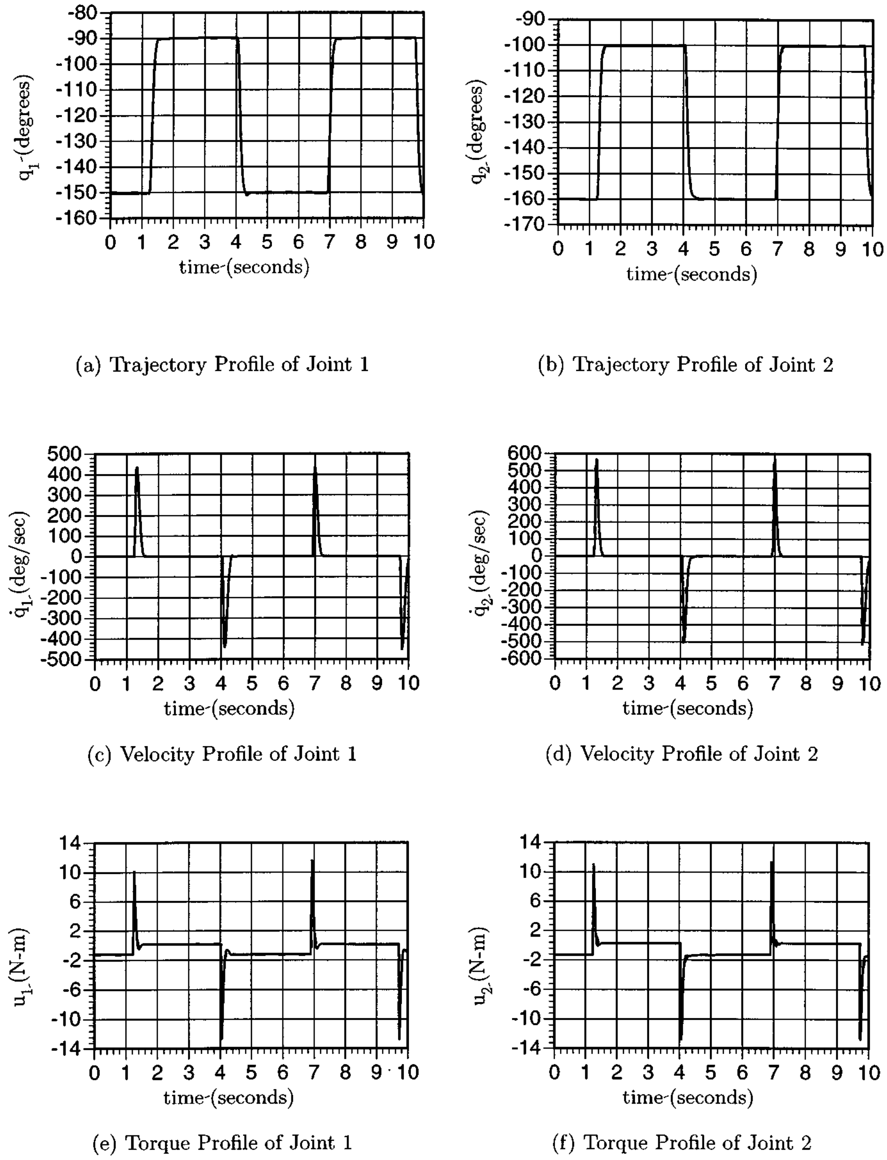

Fig. 10. Repetitive point to point motion: simulation (dashed) and experimental (solid) results: (a) trajectory profile of Joint 1, (b) trajectory profile of Joint 2, (c) velocity profile of Joint 1, (d) velocity profile of Joint 2, (e) torque profile of Joint 1, and (f) torque profile of Joint 2.

by iteratively solving for zeros of nonlinear functions) in a fraction of the sampling period. Even though the numerical computation is well posed, it still needs to be performed quite fast.

The control law presented in this paper for the regulation problem, which is originally proposed for open-chain mechanisms, evades the need for on-line computation of the implicit expressions of the model. We also showed that the proposed reduced model satisfies a skew symmetry property similar to open kinematic chains. It followed that PD-based control with simple gravity compensation (in which the gravity vector is computed at the desired constant configuration) guarantees asymptotic stability. This stability result is local, though, because of the local nature of the domain of definition of the reduced model.

We have experimentally validated the results of this paper using the RPDR which was designed and built at Rice University as a test-bed to perform control experiments on closed-chain mechanisms. Explicit equations of motion of the RPDR were obtained which still allowed us to illustrate the general modeling and control ideas presented in this paper for more general closed-chain mechanisms. Furthermore, the explicit equations enabled us to completely characterize the full domain of definition of the model and consequently to compare with the results obtained in the paper that estimate the boundaries of this domain.

Work is in progress to address the tracking problem in which the on-line computation of the implicit parts of the model will be mandatory. The issues that need to be addressed are basically first the mathematical ability to characterize a sizable domain of definition of the model where tracking is performed, and second the consequences of errors in computing the implicit expression of the model in terms of stability and performance.

REFERENCES

[1] C. Abdallah, D. Dawson, P. Dorato, and M. Jamshidi, "Survey of robust control for rigid robots," *IEEE Contr. Syst. Mag.*, pp. 24–30, Feb. 1991.

[2] Y. Amirat, G. F. Francois, J. Pontnau, and M. Dafaoui, "Design and control of a new six-DOF parallel robot: Application to equestrian gait simulation," *Mechatronics*, vol. 6, no. 2, pp. 227–239, 1996.

[3] T. Arai, R. Stoughton, and J. Merlet, "Teleoperator assisted hybrid control for parallel link manipulator and its application to assembly task," in *Proc. 2nd Int. Symp. Measurement Contr. Robot.*. Tsukuba, Japan, Nov. 15–19, 1992, pp. 817–822.

[4] S. Arimoto and F. Miyazaki, "Stability and robustness of PID feedback control of robot manipulators of sensory capability," in *1st Int. Symp. Robot. Res.*, M. Brady and R. P. Paul, Eds. Cambridge, MA: MIT Press, 1984, pp. 783–799.

[5] S. Babaci, Y. Amirat, J. Pontnau, and C. Francois, "Fuzzy adaptation impedance of a 6 dof parallel robot application to peg in hole insertion," in *Proc. 5th IEEE Int. Conf. Fuzzy Syst.*, New Orleans, LA, Sept. 1996, pp. 1770–1776.

[6] P. Bégon, F. Pierrot, and P. Dauchez, "Fuzzy sliding mode control of a fast parallel robot," in *Proc. IEEE Int. Conf. Robot. Automat.*, 1995, pp. 1178–1183.

[7] H. Brauchli and R. Weber, "Dynamical equations in natural coordinates," *Comput. Methods Appl. Mech. Eng.*, vol. 91, pp. 1403–1414, 1991.

[8] H. Brauchli, "Mass-orthogonal formulation of equations of motion for multibody systems," *J. Appl. Math. Phys. (ZAMP)*, vol. 42, pp. 169–182, 1991.

[9] R. Clavel, "Delta, a fast robot with parallel geometry," in *Proc. Int. Symp. Ind. Robot.*, Lausanne, Switzerland, Apr. 1988, pp. 91–100.

[10] O. Chételat and F. Ghorbel, "Kinematics and dynamics of the planar delta robot," Int. Rep, Institut d'Automatique, EPFL, Lausanne, Switzerland, 1994.

[11] O. Chételat, J.-P. Merlet, P. Myszkorowski, and R. Longchamp, "Algorithmes itératifs à convergence démontrée pour les changements de coordonnées des mécanismes articulés," Int. Rep. IA-96-7, Institut d'Automatique, EPFL, Lausanne, Switzerland, 1996.

[12] ——, "Globally convergent iterative algorithms for the coordinate transformations in the articulated mechanisms," in *Proc. SYROCO Symp.*, Nantes, 1997.

[13] O. Chételat, "Algorithme numérique pour les changements de coordonnées des mécanismes articulés," Ph.D. disseration, Ecole Polytechnique Fédérale de Lausanne, Switzerland, 1997.

[14] "dSPACE digital signal processing and control engineering GmbH," Technologiepark 25, Paderborn, Germany, 1993.

[15] A. Fattah, J. Angeles, and A. K. Misra, "Dynamics of a 3-DOF spatial parallel manipulator with flexible links," in *Proc. IEEE Int. Conf. Robot. Automat.*, 1995, pp. 627–632.

[16] M. Gautier, P. Khalil, and P. Restrepo, "Identification of the dynamic parameters of a closed-loop robot," in *Proc. IEEE Int. Conf. Robot. Automat.*, 1995, pp. 3045–3050.

[17] Z. Geng, L. S. Haynes, J. D. Lee, and R. L. Carrol, "On the dynamic model and kinematic analysis of a class of Stewart platforms," *Robot. Auton. Syst.*, vol. 9, pp. 237–254, 1992.

[18] Z. Geng and L. S. Haynes, "Dynamic control of a parallel link manipulator using a CMAC neural network," *Comput. Elect. Eng.*, vol. 19, no. 4, pp. 265–276, 1993.

[19] F. Ghorbel, "Adaptive control of flexible joint robot manipulators: A singular perturbation approach," Ph.D. dissertation, Dept. Mech. Eng., Univ. Illinois, Urbana-Champaign, 1990.

[20] ——, "Modeling and PD control of closed-chain mechanical systems," in *Proc. 34th IEEE Conf. Decision Contr.*, New Orleans, LA, Dec. 13–15, 1995, pp. 540–542.

[21] F. Ghorbel and R. Gunawardana, "A uniform bound for the Jacobian of the gravitational force vector for a class of robot manipulators," *J. Dynamic Syst., Measurement, Contr.*, vol. 119, pp. 110–114, Mar. 1997.

[22] F. Ghorbel, B. Srinivasan, and M. W. Spong, "On the uniform boundedness of the inertia matrix of serial robot manipulators," *J. Robot. Syst.*, vol. 15, no. 1, pp. 17–28, Jan. 1998.

[23] R. Gunawardana and F. Ghorbel, "On the boundedness of the Hessian of the potential energy of robot manipulators," *J. Robot. Syst.*, 1999.

[24] ——, "On the uniform boundedness of the Coriolis/centrifugal terms in the robot equations of motion," *Int. J. Robot. Automat.*, 1999.

[25] C. M. Gosselin, "Parallel computational algorithms for the kinematics and dynamics of parallel manipulators," in *Proc. IEEE Int. Conf. Robot. Automat.*, 1993, pp. 883–888.

[26] D. T. Greenwood, *Classical Dynamics*. Englewood Cliffs, NJ: Prentice-Hall, 1977.

[27] J. C. Hudgens and D. Tesar, "A fully parallel six degree-of-freedom micromanipulator: Kinematic analysis and dynamic model," in *Proc. ASME Des. Eng. Div. Publ. DE Trends Developments Mechanisms, Machines, Robots*, vol. 15-3, Kissimmee, FL, 1988, pp. 29–37.

[28] S. Ichiraku, "A note on global implicit function theorems," in *Proc. IEEE Int. Symp. Circuits Syst.*, 1985.

[29] C. Innocenti and V. Parenti-Castelli, "Singularity-free evolution from one configuration to another in serial and fully-parallel manipulators," *ASME Robot., Spatial Mechanisms Mechanical Syst.*, vol. 45, pp. 553–560, 1992.

[30] Z. Ji, "Study of the effect of leg inertia in Stewart platforms," in *Proc. IEEE Int. Conf. Robot. Automat.*, 1993, pp. 121–126.

[31] H. J. Kang and R. A. Freeman, "An interactive software package (MAP) for the dynamic modeling and simulation of parallel robotic systems including redundancy," in *Proc. ASME Int. Comput. Eng. Conf. Exposition*, Boston, MA, 1990, pp. 117–122.

[32] H. K. Khalil, *Nonlinear Systems*, 2nd ed. Englewood Cliffs, NJ: Prentice-Hall, 1996.

[33] J. F. Kleinfinger and W. Khalil, "Dynamic modeling of closed-loop robots," in *Proc. 16th Int. Symp. Ind. Robots*, Brussels, Belgium, 1986, pp. 401–412.

[34] T. Kokkinis and R. Stoughton, "Dynamics and control of closed-chain robot arms with application to a new direct-drive robot arm," *Int. J. Robot. Automat.*, vol. 6, no. 1, 1991.

[35] Y. Konishi, T. Aoyama, and I. Inasaki, "Learning control of a parallel-link direct-drive robot manipulator," *Robot. Auton. Syst.*, vol. 5, pp. 127–134, 1989.

[36] M. S. Konstantinov, Z. M. Sotirov, V. B. Zamanov, and D. N. Nenchev, "Force feedback control of parallel topology manipulating systems," in *Proc. 15th Int. Symp. Ind. Robot.*, 1985, pp. 181–188.

[37] F. Korrami and U. Özgüner, "Decentralized control of robot manipulators via state and proportional-integral feedback," in *IEEE Conf. Robot. Automat.*, Philadelphia, PA, 1988, pp. 1198–1203.

[38] J. D. Lee, "Optimal control of a flexible parallel link robotic manipulator," *Comput. Struct.*, vol. 48, no. 3, pp. 375–385, 1993.

[39] J. D. Lee and Z. Geng, "A dynamic model of a flexible stewart platform," *Comput. Struct.*, vol. 48, no. 3, pp. 367–374, 1993.

[40] K. Lee and K. S. Dharman, "Dynamic analysis of a three-degrees-of-freedom in-parallel actuated manipulator," *J. Robot. Automat.*, vol. 6, 1988.

[41] S. Lin, "Dynamics of the manipulator with closed chains," *IEEE Trans. Robot. Automat.*, 1990.

[42] J. Y. S. Luh and Y. Zeng, "Computation of input generalized forces for robots with closed kinematic chain mechanisms," *IEEE J. Robot. Automat.*, 1985.

[43] J. Merlet, "Force-feedback control of parallel manipulators," *Trans. IEEE Int. Conf. Robot. Automat.*, pp. 1484–1489, 1988.

[44] J.-P. Merlet, *Les Robots Parallèles*. Paris, France: Hermés, 1990.

[45] J. J. Murray and H. Lovell, "Dynamic modeling of closed-chain robotic manipulators and implications for trajectory control," *IEEE Trans. Robot. Automat.*, vol. 5, 1989.

[46] Y. Nakamura and M. Ghodoussi, "Dynamics computation of closed-link robot mechanisms with nonredundant and redundant actuators," *IEEE Trans. Robot. Automat.*, vol. 5, 1989.

[47] P. E. Nikravesh and G. Gim, "Systematic construction of the equations of motion for multibody systems containing closed kinematic loops," in *Proc. ASME Design Tech. Conf.—15th Design Automat. Conf.*, Montreal, PQ, Canada, 1989, pp. 27–33.

[48] R. Ortega and M. W. Spong, "Adaptive motion control of rigid robots: A tutorial," in *Proc. 27th Conf. Decision Contr.*, Austin, TX, Dec. 1988, pp. 1575–1584.

[49] J. E. Omri and P. Wenger, "A general criterion for the identification of nonsingular posture changing 3-dof manipulators," in *Computational Kinematics*, J.-P. Merlet and B. Ravani, Eds. Dordrecht, The Netherlands: Kluwer, 1995, pp. 153–162.

[50] A. M. Ostrowski, *Solution of Equations and Systems of Equations*. New York: Academic, 1966.

[51] F. Pierrot, A. Fournier, and P. Dauchez, "Towards a fully-parallel 6 dof robot for high-speed applications," in *Proc. IEEE Int. Conf. Robot. Automat.*, Sacramento, CA, Apr. 1991, pp. 1288–1293.

[52] F. J. Pooran, "Dynamics and control of robot manipulators with closed-kinematic chain mechanism," Ph.D. dissertation, Catholic Univ. Amer., Washington, DC, 1989.

[53] I. W. S and I. W. andberg, "Global implicit function theorems," *IEEE Trans. Circuits Syst.*, vol. CAS-28, Feb. 1981.

[54] M. Sofer, O. Melliger, and H. Brauchli, "Numerical behaviour of different formulations for multibody dynamics," in *Numer. Methods Eng.*, Ch. Hirsch *et al.*, Eds. New York: Elsevier, 1992, pp. 277–284.

[55] M. W. Spong, *Robot Dynamics and Control*. New York: Wiley, 1989.

[56] D. Stewart, "A platform with six degrees of freedom," in *Proc. Inst. Mech. Eng.* London, U.K., 1966, pt. I, vol. 108, pp. 371–386.

[57] S. Tadokoro, "Control of parallel mechanisms," *Advanced Robot.*, 1994.

[58] R. A. Tapia, "The Kantorovich theorem for Newton's method," *Amer. Math. Month.*, vol. 78/1.ea, pp. 389–392, 1971.

[59] A. E. Taylor and W. R. Mann, *Advanced Calculus*. New York: Wiley, 1983.

[60] Y. Ting, S. Tosunoglu, and R. Freeman, "Torque redistribution and time regulation methods for actuator saturation avoidance of fault-tolerant parallel robots," *J. Robot. Syst.*, vol. 12, no. 12, pp. 807–820, 1995.

[61] P. Tomei, "Adaptive PD controller for robot manipulators," *IEEE Trans. Robot. Automat.*, vol. 7, pp. 565–570, Aug. 1991.

[62] J. J. Uicker, "Dynamic behavior of spacial linkages—Part 1: Exact equations of motion," *J. Eng. Ind.*, vol. 91, no. 1, pp. 251–258, Feb. 1969.

[63] M. Vidyasagar, *Nonlinear Systems Analysis*, 2nd ed. Englewood Cliffs, NJ: Prentice-Hall, 1993.

[64] M. W. Walker, "Adaptive control of manipulators containing closed kinematic loops," *IEEE Trans. Robot. Automat.*, vol. 6, 1990.

[65] L. T. Wang and C. C. Chen, "On the dynamic analysis of general parallel robotic manipulators," *Int. J. Robot. Automat.*, vol. 9, no. 2, pp. 81–87, 1994.

[66] J. Wittenburg, *Dynamics of Systems of Rigid Bodies*. Stuttgart, Germany: Teubner, 1977.

[67] F. Ghorbel, "Coordinated Sci. Lab. Rep. UILU-ENG-91-2225," Univ. Illinois, Urbana-Champaign, Apr. 1991.

Fathi H. Ghorbel (S'86–M'87–SM'00) was born in 1962 in Sfax, Tunisia. He received the B.S. degree with honors from Pennsylvania State University, University Park, in 1985, the M.S. degree from Carnegie Mellon University, Pittsburgh, PA, in 1987, and the Ph.D. degree from the University of Illinois, Urbana-Champaign, in 1991, all in mechanical engineering.

He is an Associate Professor at the Department of Mechanical Engineering and the Department of Bioengineering at Rice University, Houston, TX, where he is also the Director of the Dynamic Systems and Control Laboratory and the Robotics Laboratory, and the Codirector of the Biomedical Systems and Instrumentation Lab. His research includes systems and control theory, robotics, and biomedical engineering systems. He is an Associate Editor for the *International Journal of Robotics and Automation*.

Dr. Ghorbel is a Member of Sigma Xi, ASME, IFAC, SIAM, and IASTED. He is an Associate Editor for the IEEE TRANSACTIONS ON CONTROL SYSTEMS TECHNOLOGY and an Associate Editor for the IEEE Control Systems Society Conference Editorial Board.

Olivier Chételat was born in Switzerland in 1967. He received the Diploma degree in electrical engineering in 1993 and the Ph.D. degree in 1997, both in automatic control, from the Institut d'Automatique, Ecole Polytechnique Fédérale de Lausanne (EPFL), Switzerland.

His research interests are in numerical kinematics computations for articulated mechanisms including closed kinematic chains. In 1998, he worked at Johns Hopkins University, Baltimore, MD, on the protein folding problem. He is currently an Engineer in the Centre Suisse d'Electronique et de Microtechnique in Switzerland.

Ruvinda Gunawardana He received the B.S. degree in mechanical engineering from Texas A&M University, College Station, in 1992 and the M.S. degree in mechanical engineering from Rice University, Houston, TX, in 1994, where he is currently pursuing the Ph.D. degree in robotics.

Roland Longchamp (M'79) was born in Yverdon, Switzerland, in 1949. He received the Diploma degree in electrical engineering and the Ph.D. degree in control systems from the Ecole Polytechnique Fédérale de Lausanne (EPFL), Switzerland.

He was a postdoctoral Fellow at the Information Systems Laboratory, Stanford University, and also at the Coordinated Science Laboratory of the University of Illinois, Urbana-Champaign. From 1981 to 1983, he worked with Asea Brown Boveri, Turgi, Switzerland, in the field of online control of large power systems. He joined the EPFL in 1983 and is currently a Professor of automatic control. His current research interests include adaptive control, system identification, and robust control, with applications to robotics, machine tools, and industrial processing.